

## Assessing and Mitigating the Risks from Bund Overtopping

Ann Halford, DNV GL, Holywell Park, Ashby Road, Loughborough, LE11 3GR, UK.

Clive Robinson, DNV GL, Holywell Park, Ashby Road, Loughborough, LE11 3GR, UK.

Gabriele Ferrara, DNV GL, Vivo Building, 30 Stamford Street, London, SE1 9LQ, UK.

Tarek Bengherbia, DNV GL, Vivo Building, 30 Stamford Street, London, SE1 9LQ, UK.

Many atmospheric pressure storage tanks are located in bunds that are designed to retain their liquid contents if the tank fails. Although the capacity of the bund is normally designed to exceed the capacity of the tank, catastrophic failures of the tank resulting in a rapid release of its contents can overtop the bund. Even if a significant proportion of the liquid overtops the bund, the hazard distances can still be smaller than those for a tank with no bund, but greater than if all the liquid is retained within the bund. This needs to be accounted for in risk assessments, especially for risk reductions studies where increasing the height of the bund or decreasing the inventory in the tank is being considered. This paper describes a methodology to account for the effect of low wall bunds on the risks from catastrophic tank failures.

Liverpool John Moores University (LJMU) carried out laboratory scale experiments on the catastrophic failure of a tank surrounded by a vertical bund wall, and several authors have produced correlations to predict the volume of liquid which overtops the bund based on this data. Many bunds on existing sites have sloping walls, but there is significantly less data for these cases. A CFD model has been used to predict overtopping for configurations similar to those in the LJMU experiments, but with sloping bund walls. A correlation which accounts for the slope of the bund wall has been developed to predict the volume of liquid which overtops the bund, based on a combination of experimental data and CFD predictions.

Liquid spread models which can predict bund over topping are often too complicated to be incorporated in risk assessment packages. A methodology has been developed to use a simpler liquid spread model to make two separate predictions, one for the liquid retained by the bund and the second for the liquid which overtops the bund, using the overtopping correlation described above to predict the source volume of liquid for the two runs. The combined pool spread and evaporation rate from the two runs can then be used as inputs to dispersion and pool fire models. In many cases the risks are dominated by the liquid that overtops the bund, but the liquid that is retained in the bund is deeper and it can result in a longer duration vapour source or pool fire.

A worked example is presented showing the effect of the slope of the bund wall on the volume of liquid which overtops the bund. The effects of the bund on the pool fire and flash fire hazard distances are also shown. Individual and societal risks for a fictitious site with a single containment LNG tank and an oil storage tank are also presented. Strategies to mitigate the risk from bund overtopping and their effectiveness are discussed and show the advantages of a more accurate assessment.

**Keywords** Bund, Overtopping

### Introduction

Many atmospheric pressure storage tanks are located in bunds that are designed to retain their liquid contents if the tank fails. Although the capacity of the bund is normally designed to exceed the capacity of the tank, catastrophic failures of the tank resulting in a rapid release of its contents can overtop the bund.

The possibility of bund overtopping has been recognised for some time and several studies have been carried out to examine the variation of the amount of overtopping to the design of the bund. Greenspan (1981) carried out a series of small scale experiments in which the initial height of fluid and the height, radius and inclination angle of the bund were varied. Clark (2001) and Hirst (2002) derived empirical equations based on this data to enable the prediction of losses. Atherton (2005) carried out a further series of tests in which the initial height of fluid, tank radius and the height and radius of the bund were varied. Atherton (2008) then extended the work by Clark to take into account the additional data by the introduction of a number of geometry specific constants. Other authors have used more complex mathematical models to carry out predictions of overtopping. For example, Webber (2009) used a mathematical model based on Shallow Water Theory to simulate the experiments by Greenspan and Atherton and obtained very reasonable agreement with the data in most cases. The only less than satisfactory agreement was found where the liquid is expected to encounter the bund with a sufficiently high velocity that it may be turned upwards and reach a height significantly greater than that of the bund where approximations made in the derivation of the Shallow Water Equations no longer hold. Nair (2008) demonstrated the use of Computational Fluids Dynamics (CFD) to predict overtopping and investigate mitigation options such as changes to bund profiles. This paper builds upon the previous work to develop a correlation to predict the volume of liquid which overtops the bund which accounts for the slope of the bund wall. This is based on based on a combination of experimental data and CFD predictions to supplement the experimental data.

Liquid spread models which can predict bund over topping are often too complicated to be incorporated in risk assessment packages. A methodology has been developed to use a simpler liquid spread model to make two separate predictions, one for the liquid retained by the bund and the second for the liquid which overtops the bund, using the overtopping correlation described above to predict the source volume of liquid for the two runs. The combined pool spread and evaporation rate from the two runs can then be used as inputs to dispersion and pool fire models. A worked example is presented showing

the effect of the slope of the bund wall on the volume of liquid which overtops the bund. The effects of the bund on the pool fire and flash fire hazard distances are also shown. Individual and societal risks for fictitious sites with single containment LNG tank and oil storage tanks are also presented. Strategies to mitigate the risk from bund overtopping and their effectiveness are discussed and show the advantages of a more accurate assessment.

## Code Requirements

An overview of general requirements for bunding can be found in Mannan (2005) in which it is stated that there is considerable arbitrariness and some inconsistency. The capacity and permitted wall height are amongst these requirements. With regard to this paper and LNG two of the most relevant standards are EN 1473 (BS EN (2007)) and NFPA 59A (National Fire Protection Agency (2013)).

EN 1473 requires impounding areas for cylindrical single containment tanks. The impounding area within the bund walls must be large enough to contain at least 110 % of the gross liquid capacity of the biggest tank within the bund. There are no other requirements relating the dimensions of the bund to the tank dimensions and there is no discussion relating to the failure mode of the tank and bund design. Therefore, although the bund design may be adequate for small spills, or spills that occur slowly, it may not retain the full tank contents in the event of a catastrophic tank failure.

NFPA 59A has more specific requirements for the bund capacity. Impounding areas serving one LNG container shall have a minimum volumetric holding capacity,  $V$ , that is one of the following:

- 1)  $V = 110$  percent of the maximum liquid capacity of the container
- 2)  $V = 100$  percent where the impoundment is designed to withstand the dynamic surge in the event of catastrophic failure of the container
- 3)  $V = 100$  percent where the height of the impoundment is equal to or greater than the container maximum liquid level

The impounding wall height and the distance from containers is determined in accordance with Figure 1 where  $X$  equals or exceeds the sum of  $Y$  plus the equivalent head in LNG of the pressure in the vapor space above the liquid. The basis for the proximity criterion is not given. However, if a release from a small hole in the tank is assumed to follow the same trajectory as an object obeying Newtonian mechanics, the maximum horizontal distance that the object could travel before dropping below the height of the bund would be equal to  $Y$  plus the equivalent head.

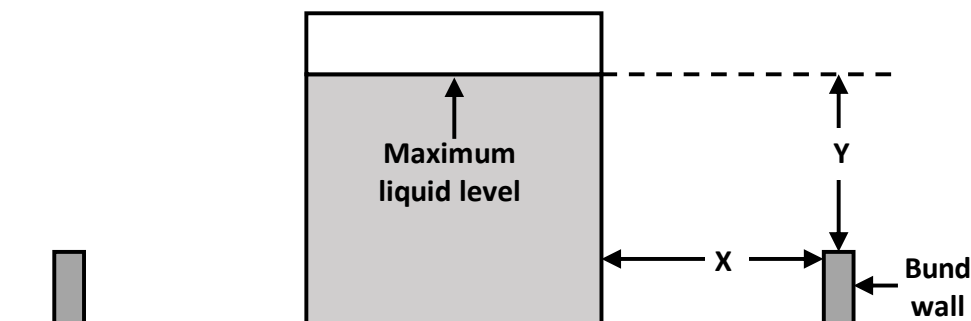


Figure 1 Impoundment Wall Proximity to Containers.

The requirements of EN1473 and NFPA 59A are compared to the cases analysed late in this paper.

## Simple Risk Assessment of an Example Site

To demonstrate the effect of bunds on the risks to people a risk assessment has been carried out for the catastrophic failures of the tanks on two example sites using two very simple assumptions. Firstly all the liquid the liquid is retained within the bund and secondly assuming that the bund has no effect, and the liquid spread is unrestricted, as it would be on flat terrain. Figure 2 shows the two example sites. The sites are very simple, one has a single LNG storage tank with a maximum capacity of 50,000m<sup>3</sup> and a radius of 25m, which is surrounded by a bund with a radius of 60m, a slope of 45° and a capacity of 110% of the maximum capacity of the tank. The maximum depth of liquid in the tank is 25.5m and the height of the bund is 4.9m. Hence, the distance  $X$  in Figure 1 is 35.0m and  $Y$  is 20.6m. Since the pressure in the vapour space is unlikely to exceed 100mbar, or 2.3m head of LNG, this configuration satisfies NFPA 59A. The second site has 4 smaller oil storage tanks, each with a capacity of 10,000m<sup>3</sup> and a radius of 15m. Each oil tank is surrounded by a bund with a radius of 40m, a slope of 45° and a capacity of 110% of the maximum tank capacity. The maximum depth of liquid in the tank is 14.1m and the height of the bund is 3.9m.

During the working day there are 20 people on each site, 15 inside a control room and 5 outdoors in a process area on the site. There is a small industrial area with a daytime population of 200 approximately 300m to the East of the LNG site 50m from the Oil site. There is a larger industrial area with a daytime population of 4000 approximately 600m to the South of the sites. There is a town to the North of the site, with its outskirts approximately 2500m from the sites which has a mean population density of 10 people/hectare, which extends indefinitely to the North.

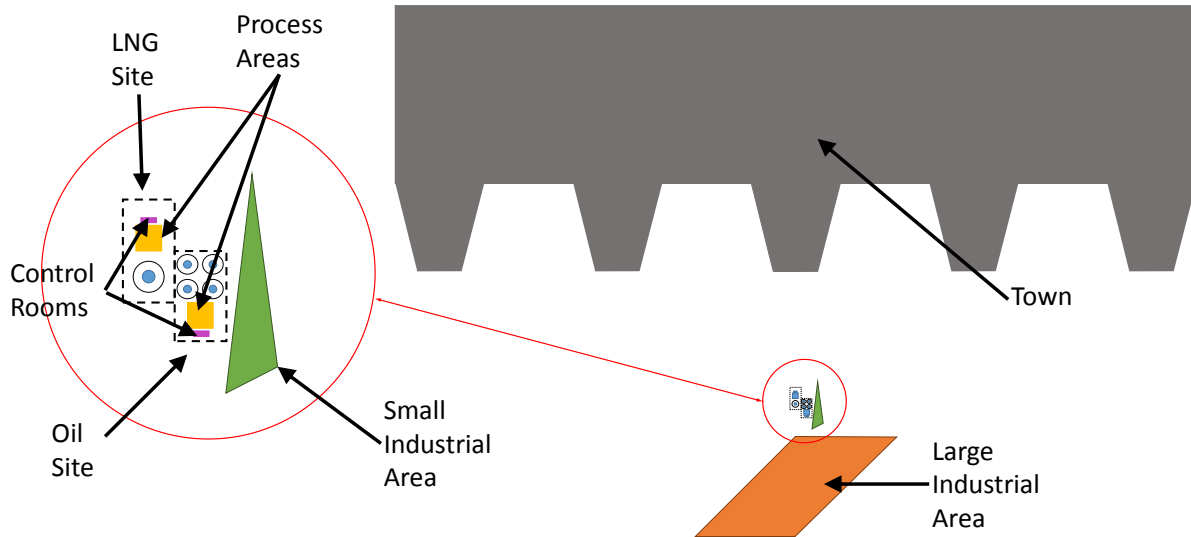


Figure 2 Two simple fictitious sites, one storing LNG and one storing oil.

It was assumed that the tanks were equally likely to fail when they contained 25, 50, 75 and 100% of their maximum capacity. Many sites cyclically fill and empty tanks, for example, sites offering seasonal storage which are filled in the Summer and emptied over the Winter, or import terminals where the tanks are rapidly filled from ships, and then gradually emptied over a longer period as the fuel is used. Assuming the tank can fail at a range of inventories would be appropriate for these types of sites. Failure frequencies of  $5 \times 10^{-7}$  per year and  $5 \times 10^{-6}$  per year and has been assumed for the LNG tank and oil tanks respectively.

Figure 3 shows the predicted FN curves for the two sites. The figure also shows an “Unacceptable” criterion line, which has a slope of -1 and passes through the R2P2 point HSE 2001, of 50 fatalities once every 5,000 years, and a “Tolerable” criterion which is two orders of magnitude lower. These criteria apply to the overall risks from the site, but they are included in the figure to give an indication of the scale of the risks from the storage tanks.

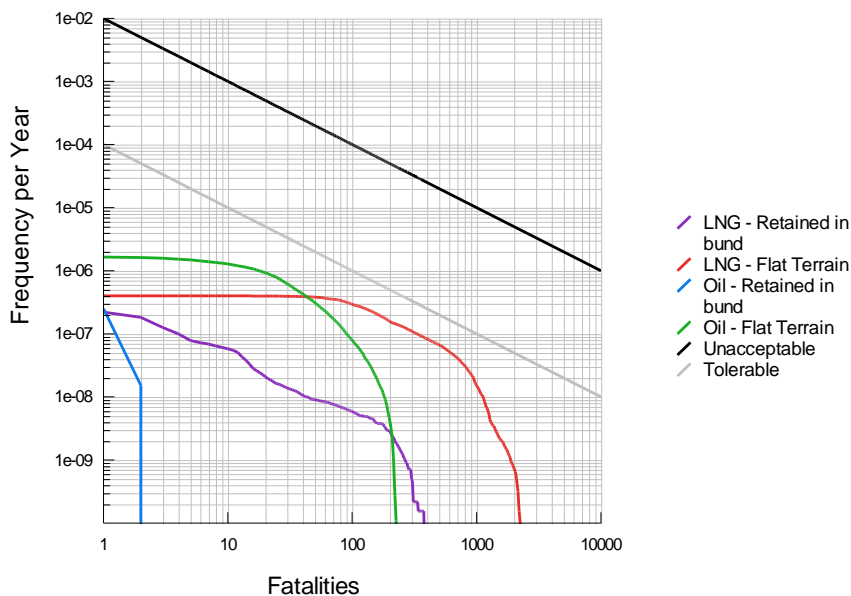


Figure 3 FN curves for tank failures on the two sites, assuming that either all of the liquid is retained in the bund or the bund has no effect and the liquid spreads as it would on flat terrain

The PLLs (Potential Loss of Life) for the LNG tank failure are  $2.7 \times 10^{-6}$  and  $1.1 \times 10^{-4}$  fatalities per year and assuming the liquid is all retained by the bund or spreads without restriction respectively, a difference of approximately a factor of forty. The corresponding PLLs for the four oil tanks are  $2.7 \times 10^{-7}$  and  $5.3 \times 10^{-5}$  fatalities per year, a difference of approximately a factor of two hundred.

Figure 4 shows the individual risks to workers on the LNG site, the oil site and the industrial area to the East of the sites. These workers are assumed to spend 42 hours per week at work, with half the time spent outdoors. As would be expected for such low frequency, high consequence events, the individual risks are relatively small, although the risks from the oil tanks are close to the tolerable if ALARP risk band for onsite workers.

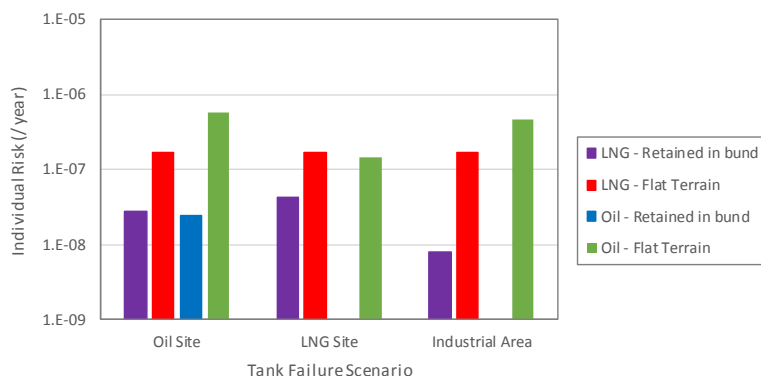


Figure 4 Individual risks for tank failures on the two sites, assuming that either all of the liquid is retained in the bund or the bund has no effect and the liquid spreads as it would on flat terrain

These figures demonstrate the sensitivity of the risk predictions to the assumptions used when modelling the effects of the bunds around the tanks.

## Experimental Data

### Greenspan and Johansson

The small scale data reported by Greenspan (1981) includes 59 experiments involving the catastrophic failure of a tank. These experiments fall into 9 groups, where only the height of the liquid in the tank is varied in each group, with the radius of the tank and the radius, height and angle of the bund wall remaining constant. As noted above, many sites cyclically fill and empty their tanks, and these tests provide useful data for the variation of overtopping with the volume of liquid in the tank.

Figure 5 shows the variation of the measured fraction of liquid which overtops the bund with the volume of liquid released, expressed as a fraction of the volume of the bund, for the 4 groups of tests where the bund walls were vertical. For typical low wall bunds satisfying NFPA 59A, this fraction will be less than 0.909.

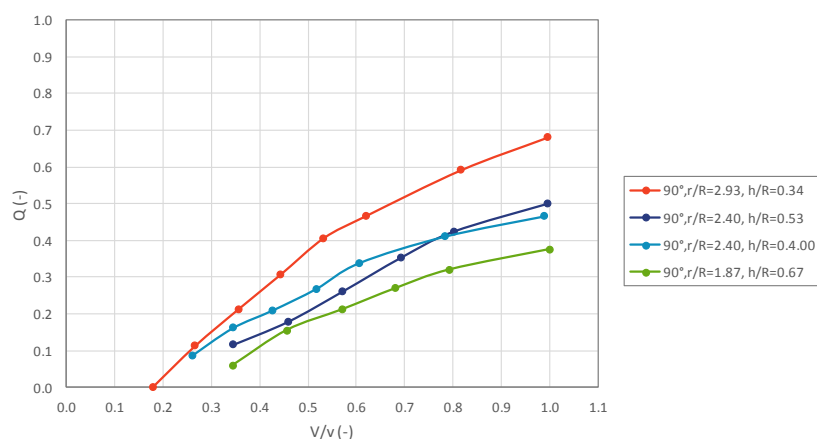


Figure 5: Variation of overtopping with liquid volume for Greenspan (1981) experiments with a vertical bund wall

In this figure,  $Q$  is the fraction of liquid overtopping the bund,  $r$  and  $h$  are the radius and height of the bund, and  $v$  is its volume.  $R$  is the radius of the tank,  $H$  is the height of liquid in the tank and  $V$  is the volume of liquid in the tank. These experiments depend on four lengths,  $r$ ,  $h$ ,  $R$  and  $H$ , and as other authors have noted, it is likely that  $Q$  will depend on three independent dimensionless combinations of these lengths.

### Liverpool John Moores University - Atherton (2005)

This data is from laboratory scale experiments at a slightly larger scale than those described in the previous section, with a tank diameter of 300mm compared to the 95mm diameter tank used by Greenspan and Johansson. The bund capacities in the experiments are between 110% and 200% of the liquid volume, covering a smaller range than the Greenspan and Johansson data. However, the experiments cover a wider range of bund sizes. There are 84 experiments with circular bunds, 24 for high wall bunds, where the bund height is greater than the liquid height in the tank and 60 for low wall bunds where the bund height is significantly smaller than the liquid height. Only the latter have been considered here. For the 60 low wall bunds, there are 15 experiments for each of the bund capacities, with three aspect ratios of the liquid source,  $H/R$  combined with five aspect ratios of the bund,  $r/h$ . Figure 6 shows the measured overtopping for the 15 cases where the bund capacity is 110% of the volume of liquid in the tank, plotted against the ratio of the bund and tank radii,  $r/R$ . This dimensionless parameter was found to have a significant effect on the volume of liquid overtopping the bund in the Greenspan and Johansson data where the bund capacity was approximately 100% of the liquid volume. Values of overtopping are also shown for the Greenspan and Johansson experiments, with the overtopping that would occur for a bund capacity of 110% estimated by interpolating between experiments.

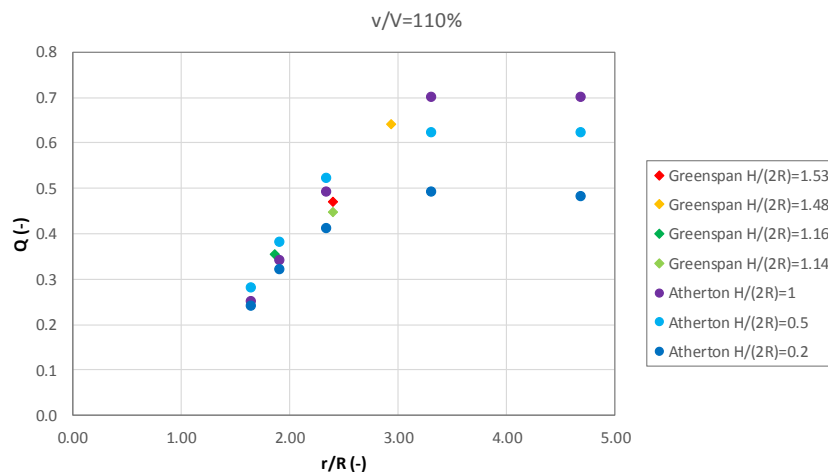


Figure 6 Variation of overtopping with the ratio of the bund radius and the tank radius,  $r/R$  for a bund capacity 110%

The combined data from the two sets of experiments have been fitted with a correlation of the form

$$Q = \text{Min} (a + b \ln (V/v), c + d \ln (V/v))$$

where  $a + b \ln (V/v)$  is a fit to the data for lower values of  $r/R$  and  $c + d \ln (V/v)$  is a fit to the data for larger values of  $r/R$ . For fixed inventories and aspect ratios of the liquid source  $a$  and  $b$  vary linearly with  $r/R$  and  $c$  and  $d$  are independent of  $r/R$ . The variation with tank fill is assumed to be accounted for in the  $\ln(V/v)$  term, with the factors  $a$ ,  $b$ ,  $c$  and  $d$  depending on dimensionless combinations of  $r$ ,  $R$  and  $h$  only.

An overall comparison of the correlation with all the Greenspan and Atherton vertical bund wall tests is shown in Figure 7, including experiments with all values of  $r/R$ .

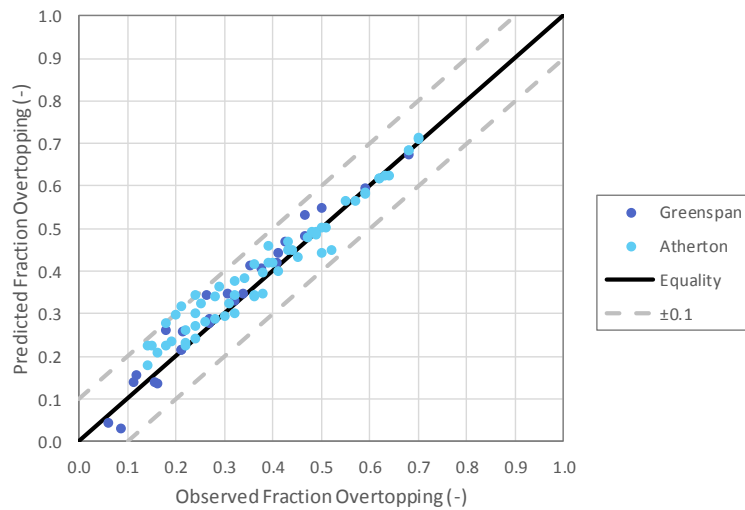


Figure 7 Comparison of the observed and predicted overtopping for all vertical bund wall experiments

**Sloping Bund Walls**

The Greenspan and Johansson data contain some experiments with sloping bunds at 30° and 60° to the horizontal. There are three groups of experiments with 60° bund walls, which have the same tank radius, bund height and bund radius as three of the groups of experiments with vertical bund walls. There are also two groups of experiments with 30° bund walls. Figure 8 shows a comparison of the overtopping from six groups of tests, comparing groups where the only difference is the slope of the bund wall.

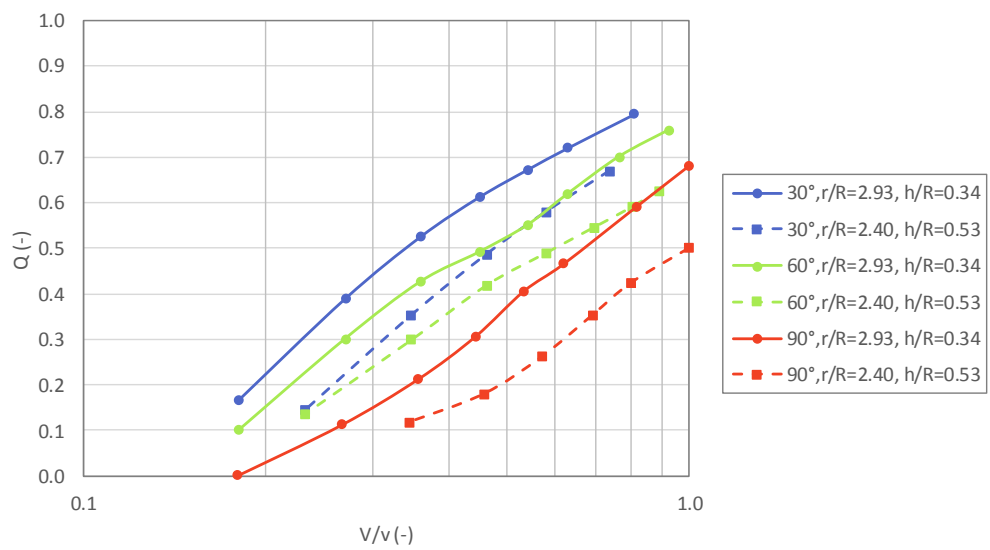


Figure 8 Variation of overtopping with bund slope and capacity

This shows that there is greater overtopping for bund walls with a shallower slope. Each group of tests was fitted to a correlation of the form  $A + B \ln(V/v)$ , and the constants A and B were compared for groups of experiments where only the slope of the bund wall varied. This analysis suggested that the slope of the bund wall had a greater effect on the parameter A and a smaller effect on the parameter B. This was confirmed by comparing a correlation for the vertical bund wall experiments of Greenspan and Johansson to all of their experiments, as shown in Figure 9.

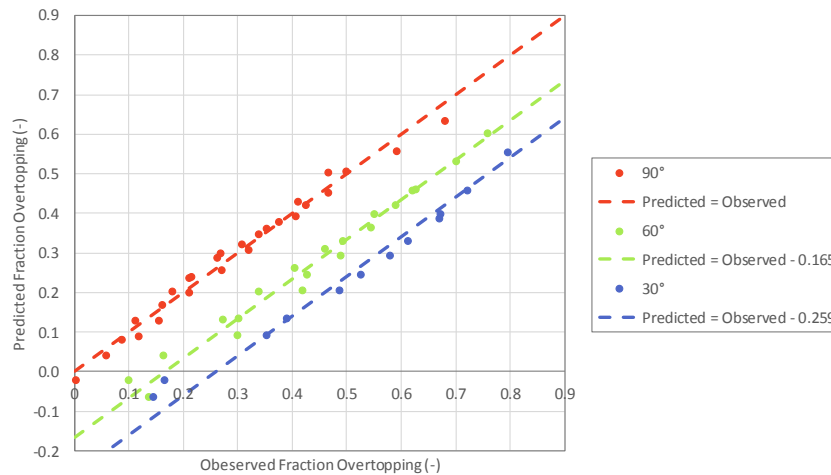


Figure 9 Comparison of the observed overtopping with a correlation for vertical bund walls

This suggests that in the parameter ranges of these experiments, an additional fraction of 0.165 overtops bunds with a slope of 60° and an additional fraction 0.259 overtops bunds with a slope of 30°. In the absence of experimental data it would be reasonable to interpolate between these values for bunds with slopes of between 30° and 60°.

It is likely that the additional overtopping which occurs for sloping bunds depends on parameters other than the slope of the bund wall, but this experimental data does not cover a sufficiently wide range of parameters to justify this. CFD calculations have been carried out for sloping bund walls with a wider range of parameters to extend the correlation. These are discussed in the next section.

## CFD Modelling

### Background

The modelling of liquid spreading in a bund following a catastrophic tank failure, has often been based on the so-called “shallow water” approach Ivings (2007). The shallow water equations assume that the vertical component of acceleration is negligible reducing the problem to a 2D approach (x, y). While this approach is undoubtedly attractive in terms of computational efficiency, the actual dynamics of a liquid interacting with a wall is intrinsically a 3D phenomenon with strong accelerations in the vertical direction. This calls for the need of sub-models that, in turn, require ad-hoc validation and introduce a degree of uncertainty on the actual capability of the model to capture the main physics of the phenomenon.

The CFD approach used in this paper, is based on a full 3D approach that explicitly considers the geometry of the wall avoiding the necessity of ad-hoc sub models. The model employs a multiphase approach (liquid-air) exploiting a surface-tracking technique for immiscible and not interpenetrating fluids. The approach is known as Volume of Fluids (VoF) and tracks the volume fraction (indicated with  $\alpha$  in Figure 10 of each of the fluids in each computational cell of the domain. The tracking of the interface between phases is accomplished by the solution of a continuity equation for the volume fraction of one of the phases (mass transfer from one phase to another is included via a source term). The model has been implemented in the general-purpose CFD package CFX-ANSYS.

Based on the above considerations, the VoF approach is far more computationally expensive than a shallow water approach but undisputedly more accurate. The benefits of the CFD modelling are evident when the geometry of the tank-bund assembly departs from the idealised conditions used in the scaled experiments and when the effectiveness of mitigation measures must be evaluated.

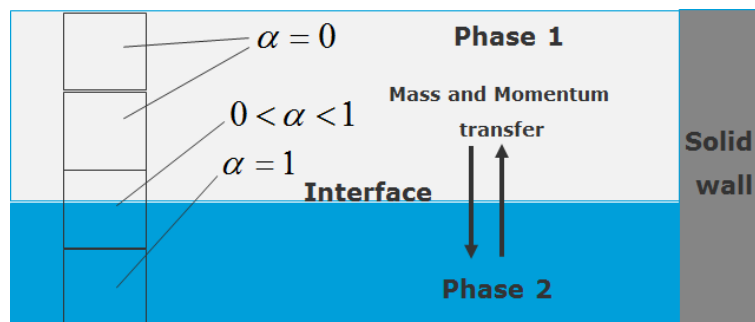


Figure 10 Schematic of the Volume of Fluid Method. The interface of the two fluids and the presence of obstacles are fully resolved and taken into account in 3D.

## Numerical Details

The numerical solutions have been obtained with a pressure-based algorithm. Second-order explicit scheme and 2nd order upwind scheme have been used to discretise the equations respectively in time and space.

The quality of the grids used in the simulations has been ensured through grid sensitivity assessments. For a reliable prediction of the liquid velocity in the bund, a fine resolution of the vertical gradients was necessary. This was ensured through the strict adhesion to the  $Y^+$  criterion (the value of the dimensionless distance from solid surfaces) which was limited to values lower than 300. Efforts were also devoted in the detailed resolution of the interface. In this case, the best strategy consisted in a dynamic resolution of the grid conditioned to the actual position of the interface.

Based on results of the grid sensitivity assessment, it was concluded that the model was characterised with an acceptable independence from the grid resolution that allowed to rule out the presence of significant numerical errors.

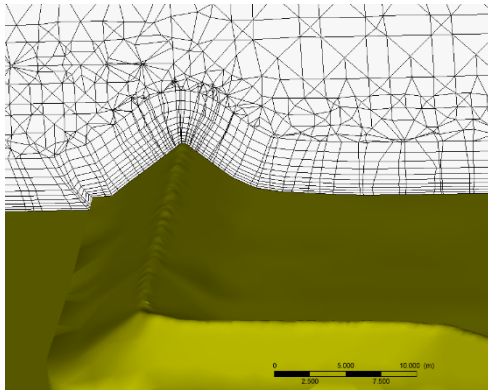


Figure 11 Details of the vertical resolution implemented in the numerical grids.

## Model Validation

Once the numerical quality of the model was ensured, the model was evaluated in terms of its capability to reproduce the reality. The model was tested against two sets of experimental data (see Figure 12):

- 1) Laboratory-scale dam break experiment. The experiment simulates a dam break where a column of water is suddenly allowed to collapse into a closed baffled vessel. This test case is considered a benchmark for validating free surface models. The developed CFD model could well reproduce the dynamics of the flow in terms of fluid velocity, wave impact on the baffle and wave reflection in the vessel.
- 2) Laboratory-scale test of catastrophic tank failures at Liverpool John Moore University (Atherton (2005))). This is one of the most comprehensive set of data that simulate the sudden and catastrophic loss of containment of a bunded tank (vertical walls) and the following overtopping of the liquid. In this case, the developed CFD model was able to well replicate the measured quantities of overtopped liquid (i.e. liquid not contained in the bund).

The agreement of the CFD model predictions with the two sets of experiments, in both qualitative and quantitative terms, was satisfactory enough to provide reasonable confidence in the results obtained with different inclinations of the bund wall.



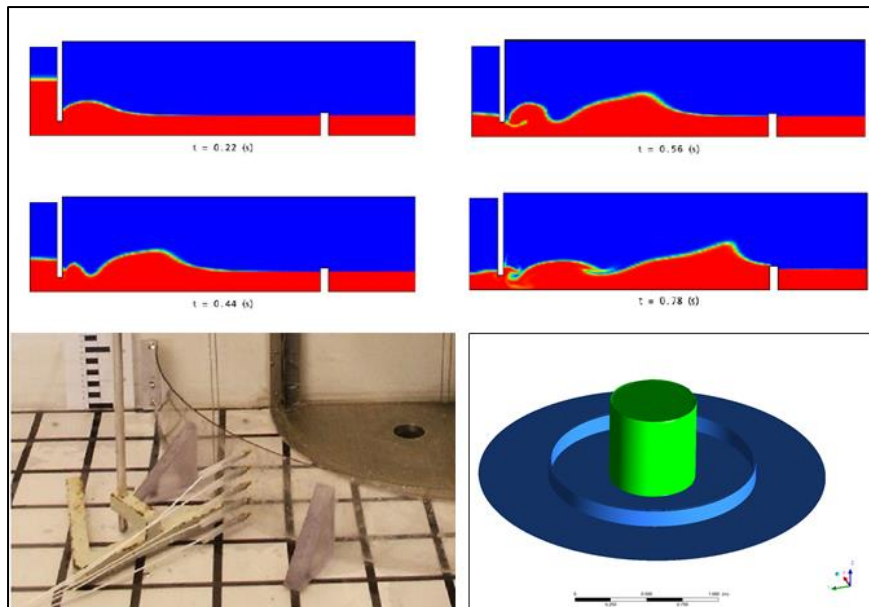


Figure 12 Top: Dam-break experiment results as reproduced by the CFD model at several times. Bottom: Experimental setup of the Liverpool John Moore University tests and CFD model..

### Extended Correlation for Sloping Bund Walls

The CFD predictions for bund walls with a slope of 30° have been compared to Atherton’s data for experiments with the same bund and tank dimensions, and the additional volume of liquid which overtops the bund calculated. Similar comparisons were also made for the Greenspan experiments, using a fit to the data to make estimate the additional overtopping for bund capacities of 110% and 220%. The CFD predictions covered a wider range of parameters than the Greenspan experiments. The Greenspan data and CFD predictions have been fitted with a correlation of the form

$$dQ = e + f \theta$$

where  $dQ$  is the additional overtopping due to the sloping bund wall. As noted earlier in this paper, the Greenspan data suggests  $dQ$  does not vary with the ratio of the volume of liquid to the bund capacity,  $V/v$ , and the factors  $e$  and  $f$  depend on dimensionless combinations of  $r$ ,  $R$  and  $h$  only. Figure 13 shows a comparison of the overall model with the experimental data and the CFD predictions. In a majority of cases the correlation is within 0.1 of the data or CFD predictions.

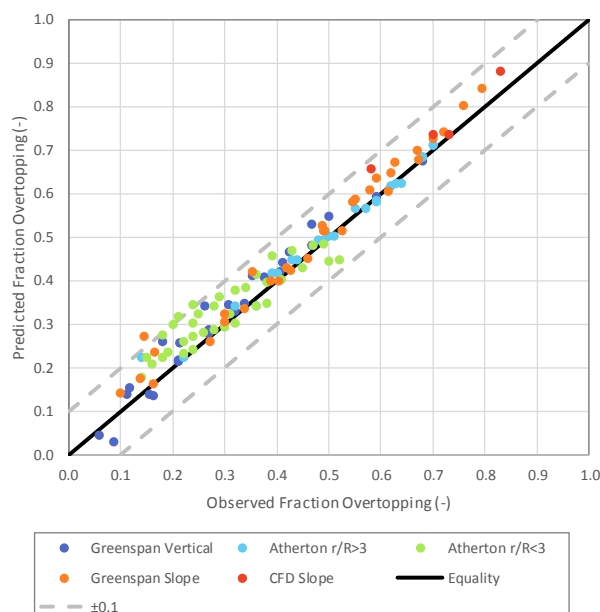


Figure 13 Comparison of the observed and predicted overtopping for all vertical bund wall experiments

## Development of Liquid Spread Model Accounting for Overtopping

The correlation described above can be used to predict the volume of liquid which overtops the bund due to the catastrophic failure of a storage tank. The effect of this on the predicted hazards and risks are also of interest, and a liquid spread model has been produced to predict the subsequent liquid spread when overtopping occurs. This model runs an existing liquid spread model several times, then combines the separate predictions to produce an overall model which accounts for the liquid retained in the bund and the liquid which overtops the bund.

First, the correlation above is used to determine whether any overtopping occurs. If overtopping occurs, the volume of liquid which overtops the bund,  $V_{\text{Over}}$ , is calculated.

$V_{\text{Over}} = Q V_{\text{Tank}}$  where  $V_{\text{Tank}}$  is the initial volume of liquid in the tank.

A liquid spread calculation is then carried out for a release onto flat terrain, and the time  $t_0$  that the predicted pool radius is equal to  $r$ , the radius of the bund, is noted. A second liquid spread calculation is then carried out for a source with a radius equal to the radius of the bund. The liquid is released from this source at a rate which decays linearly from  $w$  to zero over a time  $2\Delta t$ . To conserve the volume of liquid,  $V_{\text{Over}} = w \Delta t$ . The height of the source is chosen so that the Froude number of the source for the initial flow rate is 1. This choice of height avoids numerical problems with the liquid spread model. The time over which overtopping is observed to occur is typically short, and the predicted spread is not overly sensitive to the choice of  $\Delta t$ . However, if  $\Delta t$  is too short, then this second liquid spread calculation can predict that the pool outside the bund spreads more quickly than a spill onto flat terrain. Another consideration is that some liquid spread models can become unstable for sources that have a very high flow rate for a very short duration. An estimate of the time scale over which overtopping occurs can be obtained by re-examining the initial calculation for flat terrain to find the time  $t_1$  when the predicted pool radius is equal to  $r/\sqrt{1-Q}$ . At this time a fraction  $Q$  of the pool area lies outside the bund radius  $r$ , so if the pool was a cylinder with a uniform depth, then a fraction  $Q$  of the volume would be outside the bund. The time scale of the overtopping is then assumed to be  $\Delta t = t_1 - t_0$ .

Example calculations have been carried out for the LNG tank used in the example calculations at the start of this paper, assuming that the tank is 50% full when it fails. The correlation suggests that 41% of the LNG, that is about  $10,000\text{m}^3$ , overtops the bund. The flat terrain calculations suggest that the pool first hits the bund wall 4.4 seconds after the tank fails, and 41% of the area of the pool is outside the bund after 7.1 seconds, hence  $\Delta t = 2.7$  seconds. The initial release rate used for the calculation,  $w$ , is  $3,800\text{m}^3/\text{s}$  or about  $10\text{m}^3/\text{s}$  for each unit length of the bund perimeter.

Figure 14 shows the predicted evaporation rate from inside the bund, from the liquid which overtops the bund and the combined evaporation from both areas. The figure also shows the evaporation rate for a catastrophic failure on flat terrain. Figure 15 shows the predicted pool radius for both cases.

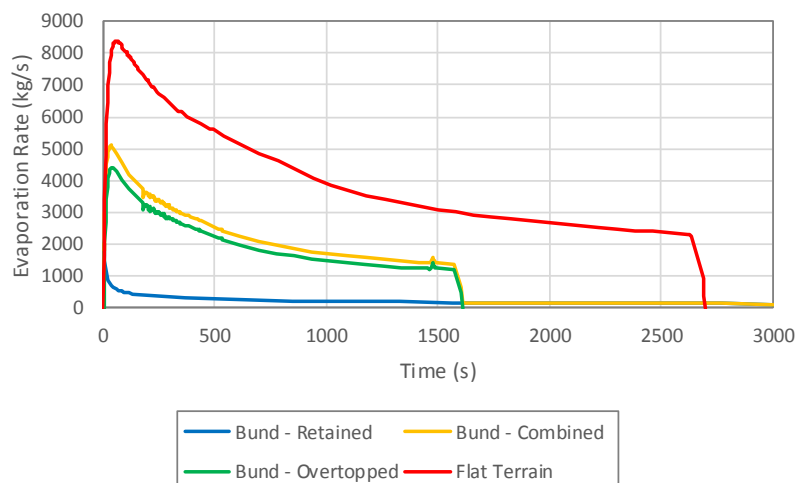


Figure 14 Predicted evaporation rate on flat terrain and accounting for a bund

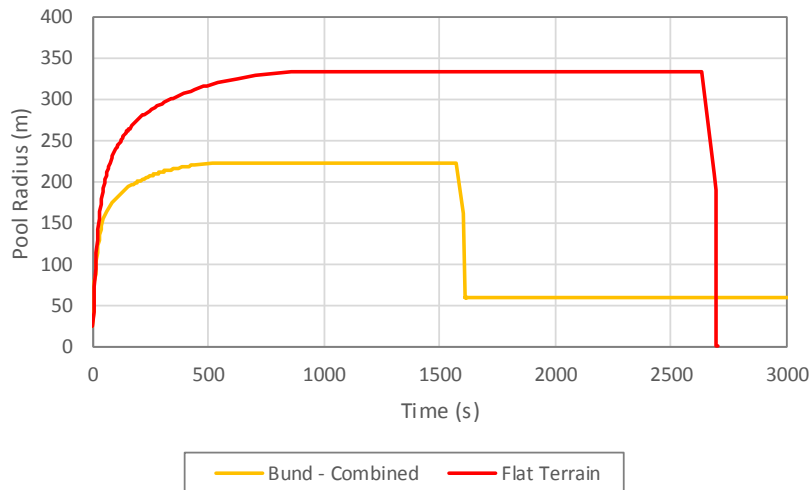


Figure 15 Predicted pool radius on flat terrain and accounting for a bund

These figures show that if the effects of the bund are accounted for there is a significant reduction in the pool radius and the maximum evaporation rate compared with a spill on flat terrain.

**Hazard Modelling**

Dispersion predictions have been made for a catastrophic failure of the LNG tank from the worked example at the start of this paper. Predictions have been made for a failure when the tank contains 100%, 75%, 50% and 25% of its maximum inventory, with the correlation predicting that 56%, 45%, 29% and 0% of the liquid would overtop the bund for the four inventories. The predicted dispersion distance to the LFL in 2F and 5D atmospheric conditions are shown in Figure 16.

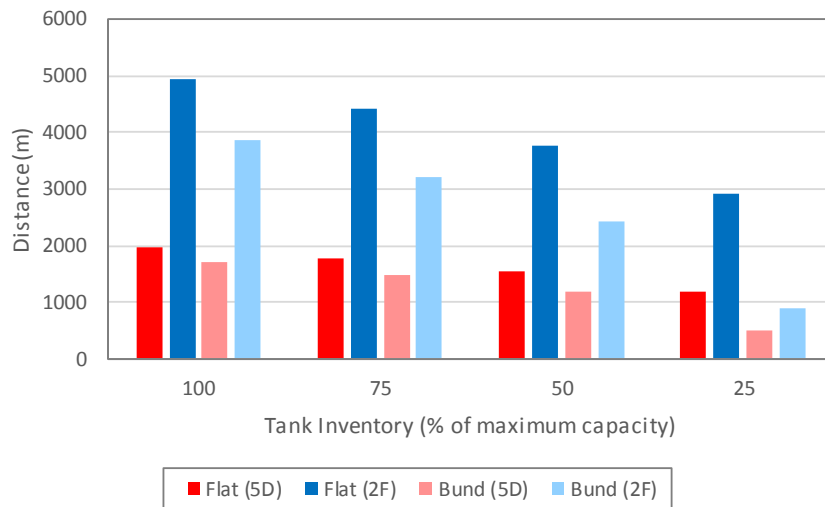


Figure 16 Predicted dispersion distance to LFL for a failure of an LNG storage tank

Fire predictions have been made for a catastrophic failure of an oil tank from the same example. The hazard distances are shown in Figure 17. The hazards from the pool fires are less sensitive to the wind speed, and the maximum hazard over all the six wind speeds used in the risk assessment is shown.

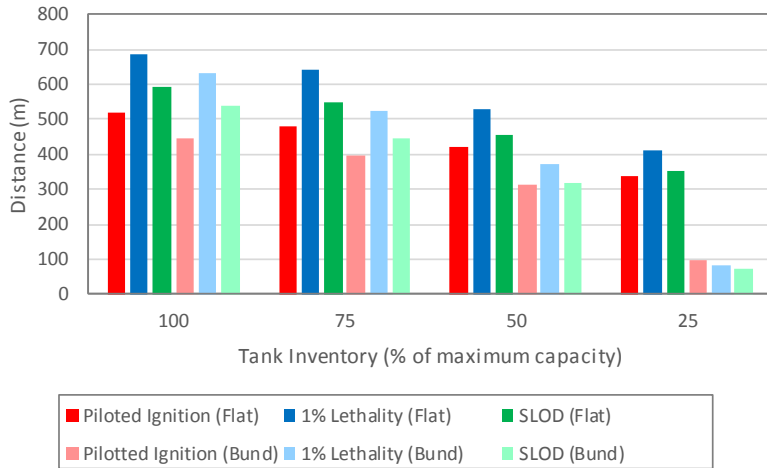


Figure 17 Predicted dispersion distance to 1% lethality, SLOD and piloted ignition for a failure of an oil storage tank

These figures show that the predicted hazard distances are smaller when the bund is accounted for. The reduction in the hazard distance is particularly noticeable for smaller inventories, where a greater proportion of the inventory is retained by the bund. In particular, the correlation predicts that no overtopping occurs when the LNG and oil tanks are 25% full, and the hazard distances accounting for the bund are very much smaller than those where the bund is assumed to have no effect for this case.

**Risk Modelling**

**Predictions for the Example Site**

The risk calculations for the LNG and oil storage sites presented at the start of the paper have been repeated. The volume of liquid predicted to overtop the bund and the subsequent spread of this liquid have been predicted using the models described in this paper. Catastrophic failures of storage tanks can be caused by external events, such as earthquakes and air crashes. These events could be so severe that they also impair the integrity of the bund. To account for this, it has been assumed that 10% of tank failures damage the bund, and it has been cautiously assumed that the remaining bund does not restrict the liquid spread, and the consequences are the same as for a tank failure with no bund. Figure 18 shows the predicted FN curves for the two sites. The figure also shows the curves for releases onto flat terrain, for comparison.

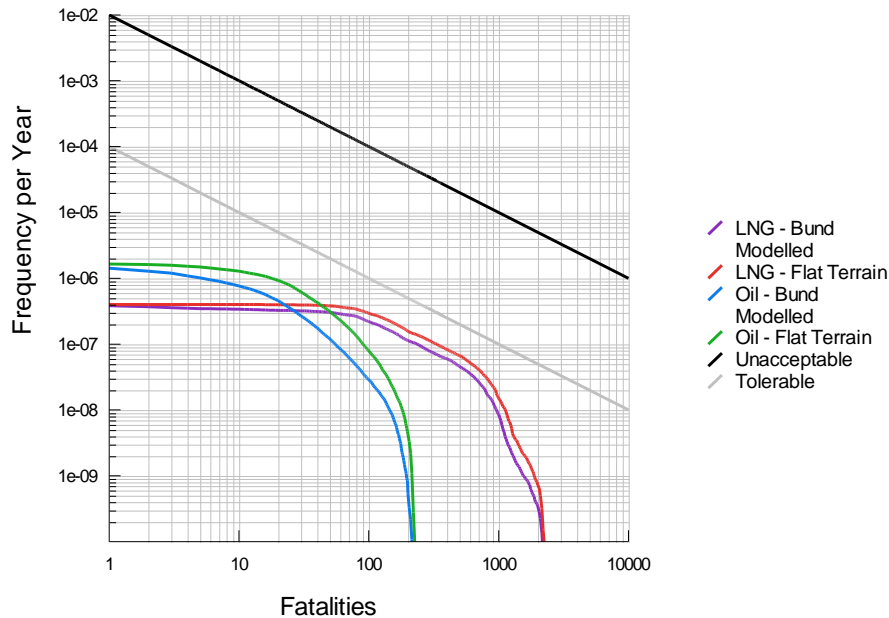


Figure 18 FN curves for tank failures on the two sites, accounting for the bund and ignoring the bund

Figure 19 shows the individual risks to workers on the LNG site, the oil site and the industrial area to the East of the sites

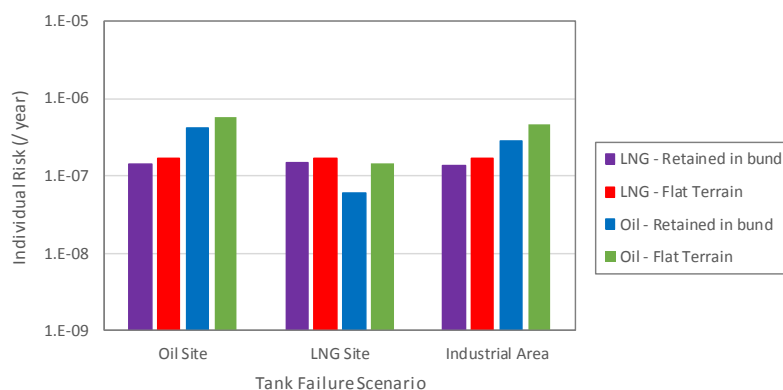


Figure 19 Individual risks for tank failures on the two sites, accounting for the bund and ignoring the bund

This shows that accounting for the effects of the bund reduces the predicted risks, with the individual risk being 40% -90% of the risks for the case with no bund.

### Risk Reduction

The models for the effects of bunds can be used in risk reduction studies. Figure 20 shows the predicted PLL (Potential Loss of Life) if the height of the bund in the previous example is increased so that the bund can hold 150% of the maximum contents of the tank, if the slope of the bund wall is increased from 45° to 60° and if the tank is operated at 80% of its maximum inventory or less. The first two might be considered when designing a new site, the last could be a risk reduction option for an existing site. The figure also shows the PLLs for the original bund design, a release onto flat terrain and a release that is contained within the bund.

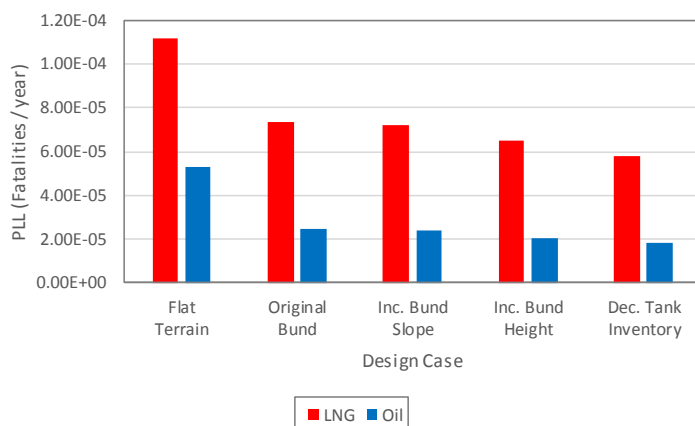


Figure 20 Comparison of the PLL for different design options

This figure shows that all the risk reduction measures considered reduce the risks from the sites compared to the original assessment. Increasing the height of the bund wall has a greater effect than increasing the slope of the bund wall.

### Discussion

Bunds surrounding atmospheric pressure storage tanks can affect the risks from a catastrophic tank failure. Example calculations show that there are large differences in the risks predicted for the most optimistic case, where all the liquid is assumed to be retained in the bund, and the most pessimistic case, where the effect of the bund is ignored. Hence, bunds are likely to have a significant effect on the risks from tank failures, and a methodology for predicting the risks from catastrophic tanks failures has been developed which takes account of the effects of bunds.

Experimental data for the overtopping of a circular vertical bund walls covers a wide range of parameters. Although many bunds on existing sites have sloping walls, the data for sloping bund walls is more limited. A CFD model has been used to generate predictions for sloping bund walls for parameter ranges where there is no experimental data. This CFD model has been validated against experimental data, and its predictions found to agree with experimental data where experimental data was available. A correlation has been developed to predict the volume of liquid which overtops a circular bund following a catastrophic tank failure, based on a combination of experimental data and CFD predictions. The predictions of the correlation vary continuously as the dimensions of the tank and bund, and the slope of the bund are varied, allowing different bund designs to be compared.

A methodology has been developed to predict the spread and evaporation of the liquid which overtops the bund. This methodology uses the correlation described above to predict the volume of liquid which overtops the bund. Separate runs of

an existing liquid spread model are used to predict the evaporating and spread of the liquid retained in the bund and the liquid which overtops the bund, and the results are then combined to give the total evaporation rate and overall pool radius.

The methodology has been used to predict the risks from an example site. The predicted risks are significantly lower than those that are predicted if the effects of the bund are ignored, and the model can account for different designs of bund.

## References

Atherton, W., 2005. An experimental investigation of bund wall overtopping and dynamic pressure on the bund wall following catastrophic failure of a storage vessel. HSE Research Report 333.

Atherton W., Ash J.W. and Alkhaddar, R.M., 2008 The Modeling of Spills Resulting from the Catastrophic Failure of Above Ground Storage Tanks and the Development of Mitigation. International Oil Spill Conference Proceedings: May 2008, Vol. 2008, No. 1, pp. 949-956.

BS EN 1473:2007, Installation and equipment for liquefied natural gas — Design of onshore installations

Clark S.O., Deaves D.M., Lines I.G. and Henson L.C., 2001, Effects of Secondary Containment on Source Term Modelling. HSE Contract Research Report 324/2001.

Greenspan, H.P., Johansson, A.V., 1981, An Experimental Study of Flow Over an Impounding Dyke, Studies in Applied Mathematics, Vol.64, 211-233.

HSE, Health and Safety Executive, Reducing Risks, Protecting People, HSE's decision-making process

Ivings, M.J. and Weber, D.M., 2007, Modelling Bund Overtopping using a Shallow Water CFD Model, Journal of Loss Prevention in the Proc. Ind. 20, 38-44, 2007.

Mannan, S. Lee's, 2005, Lee's Loss prevention in the process industries', Third Edition, Section 22.21.

Nair, S.R., 2008, Methods of Avoiding Tank Bund Overtopping Using Computational Fluid Dynamics Tool, Hazards XX, Paper 40.

NFPA 59A, 2013 Edition, Standard for the Production, Storage, and Handling of Liquefied Natural Gas (LNG),

Thyer, A.M., Hirst, I.L., Jagger, S.F., 2002, Bund Overtopping – The Consequences of Catastrophic Tank Failure, J. Loss Prev. Process Ind., 15, 357-363.

Webber, D.M. Ivings, M.J. Maru, W-A. and Thyer, A.M., 2009, Validation of the Shallow Water model "SPLOT" against experimental data on bund overtopping, HSE Research Report 755.